

# UNDULATOR COMMISSIONING FOR A HIGH-ENERGY-GAIN INVERSE FREE ELECTRON LASER EXPERIMENT

J. P. Duris, R. K. Li, P. Musumeci, E. Threlkeld

Department of Physics and Astronomy, UCLA, Los Angeles, CA 90095, USA

## Abstract

We present the construction and measurement details of a strongly tapered helical undulator for the Rubicon Inverse Free Electron Laser (IFEL) experiment. Results of the magnetic field measurements are presented, and these are used to produce simulations of the expected performance of the experiment. Finally, a study of the tolerances on the input parameters of the experiment is presented.

## INTRODUCTION

The Rubicon IFEL experiment aims to achieve energy gain and accelerating gradient significantly larger than what is possible with conventional RF accelerator technology to pave the way for applications such as a portable driver for inverse Compton sources and FELs [1]. Previous IFEL experiments at BNLs Accelerator Test Facility (ATF) [2] successfully demonstrated staging and narrow energy spread while the UCLA Neptune IFEL experiment achieved high gradient acceleration in excess of 70 MeV/m [3]. This experiment brings together these two major groups active in IFEL research and combines ATFs electron beam and high power CO<sub>2</sub> laser system with a strongly tapered helical permanent magnet undulator designed and built at UCLA to achieve high energy gradient and gain.

## UNDULATOR CONSTRUCTION

The undulator design implements the superposition of two orthogonally oriented permanent magnet Halbach undulators each with four magnets per period and shifted by a quarter of a period relative to each other. Each magnets was wire cut by the manufacturer from a large cylinder of Nd-FeB with 1.22 T magnetization into a uniform shape with different thicknesses. The pole face on one side was tapered to increase the flux density near the beam.

This is the first time a helical strongly tapered undulator has been built. The strong tapering varies the resonant energy allowing for high gradient acceleration. The helical geometry coupled with a circularly polarized laser offers near continuous acceleration as the electrons undulate in a helical motion about the undulators axis resulting in more than twice the gradient of a planar undulator. Details of the tapering optimization can be found in Reference [4]. Additionally, entrance and exit periods keep the axis of the helical motion of the electron beam centroid from deviating off axis [5].

The surfaces where the magnets and holders interface were first cleaned with acetone to remove oils. Then the

Table 1: Undulator Specifications

|                         |                 |
|-------------------------|-----------------|
| Undulator period        | 4.0 cm – 5.9 cm |
| Magnetic field strength | 5.2 kG – 7.7 kG |
| Undulator parameter K   | 1.94 – 4.26     |
| Periods                 | 11              |

holder surfaces were scored with a razor to increase the surface area available for the epoxy to bond with. The magnets were epoxied in their holders and placed in an oven for 2 hours between 50 and 60 °C and then allowed to cool for at least 48 hours. The annealing procedure was recommended by the epoxy manufacturer to increase the strength of the bond 50%, and there is evidence that thermal treatment improves the radiation resistance of NdFeB magnets [6]. The oven temperature was kept well below the Curie point of NdFeB, and the magnetization of a test magnet was found to remain unchanged even after an integrated total of more than a week of baking.

In order to maintain high vacuum, the beam is transported through a thin aluminum pipe which fits in the 15 mm gap between undulator magnet poles. The magnets polarized transverse to the beam have a large force pulling them in towards the pipe. Caps were bolted into the holders of these magnets, pinning the magnets in place to prevent catastrophic damage to the pipe in the unlikely event of an epoxy failure. The holders with attached magnets were then assembled together in modules for each period before being inserted into the undulator rails.

## FIELD MEASUREMENTS

A motorized hall probe system shown in Figure 1 was developed to automate scans of the on-axis transverse magnetic field profile. The hall probe was attached to a Teflon carriage which was driven by a stepper motor which allowed for reproducible measurement step sizes of 0.396 mm or 100 to 150 measurements per period. A fixed current source supplied the hall effect sensor with a supply of current stable to 50  $\mu$ A while a digital multimeter measured voltage to a precision of about 0.004%. The hall sensor magnetic field response was determined to be 9.00 mV/kG when calibrated with a Sypris reference magnet. Deviation from linearity in the range of 0.8kG to 9.6kG for positive and negative polarity was measured with two strong magnets arranged in a Helmholtz geometry and corrected for in the resulting scans. Measurements were automated with LabVIEW, and the final fields are depicted in Figure 3.

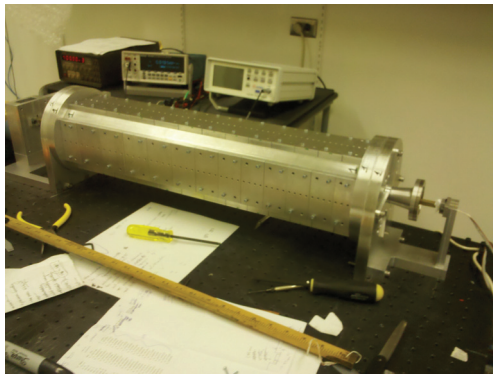


Figure 1: Undulator field scan setup.

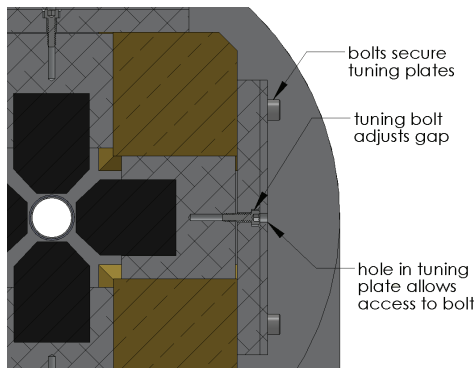


Figure 2: A cross sectional view of the undulator showing gap adjustment. The magnet sits in a slot in the rails and attaches to the tuning plate by a single bolt which can be adjusted to move the magnet in the slot.

The field scans guided the tuning. Each magnet holder was connected to plates by a single bolt as shown in Figure 2. Adjusting the bolt allows the magnet to travel in a slot in the undulator rail thereby modifying the magnet gap. Epoxy thicknesses at the holder-magnet interface varied by up to a few hundred microns so this was first measured and compensated for all magnets to ensure each magnet was equidistant from the axis. The gaps between magnets were then tuned simultaneously to achieve a better than 0.1% agreement with a RADIA simulated field profile.

Integrals of the measured fields were calculated in order to estimate the mean velocity and position of the electron beam as it traverses the undulator. It is desirable to keep the electrons from deviating too far from the axis and out of the center of the laser radiation. The largest predicted electron beam undulation radius was estimated to be about half the expected laser waist of 0.91mm. A further goal of minimizing the deflection was met, and the exit angle is estimated to be less than 1 mrad.

### EXPECTED PERFORMANCE

Simulations utilizing the measured fields of the tuned undulator were performed with the FEL simulation code Genesis 1.3. [7] Since Genesis does not allow for arbitrary

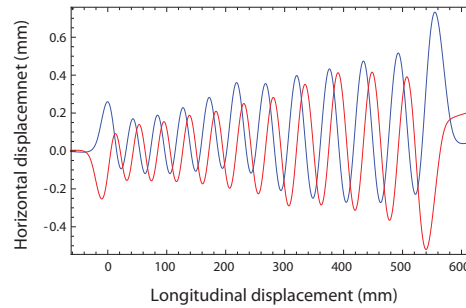
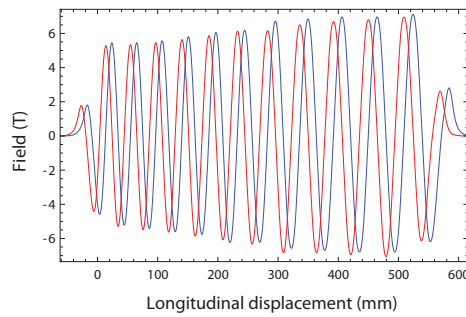


Figure 3: Field maps and integrals. The calculated particle velocities and displacements are show as well.

tapering schemes, multiple Genesis instances were chained together over the length of the undulator. [8] The simulation parameters which are expected to be used in the experiment are shown in Table 2.

Table 2: Simulation Parameters

|                        |              |
|------------------------|--------------|
| Initial energy         | 50 MeV       |
| Charge                 | 500 pC       |
| Emittance              | 2 mm-mrad    |
| Beam size at entrance  | 200 $\mu$ m  |
| Laser power            | 500 GW       |
| Laser wavelength       | 10.3 $\mu$ m |
| Rayleigh range         | 25 cm        |
| Laser waist            | 0.91 mm      |
| Optimal focal position | -10 cm       |

The resulting longitudinal phase space of the simulated output beam is shown in Figure 4. The accelerated bunch is clearly separated from the background and has a mean energy of 115 MeV with a relative energy spread of 3.8%. The simulated input beam was uniformly distributed in phase. The fraction of particles which fill the initial bucket and remain trapped was 26%, and the resulting micro bunch length was 5 fs.

Genesis can also be used for numerical studies of the time dependent IFEL interaction. Time dependence was included by dividing the beam up longitudinally by slices of the length of the laser wavelength. Figure 5 shows the results of using this method to simulate the temporal effects of the IFEL process for the parameters in Table 2. Both beam current and laser power temporal profiles were

Table 3: Simulation Results

|                           | 400 GW  | 500 GW  | 600 GW  |
|---------------------------|---------|---------|---------|
| Fraction accelerated      | 13%     | 26%     | 31%     |
| Mean final energy         | 117 MeV | 117 MeV | 115 MeV |
| Energy spread (rms)       | 2.0%    | 2.5%    | 3.8%    |
| $\mu$ -bunch length (rms) | 3.9 fs  | 4.8 fs  | 5.1 fs  |

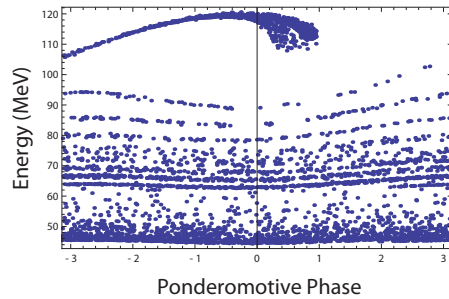


Figure 4: Longitudinal phase space of the output electrons for nominal parameters and 500GW laser power.

modeled as gaussian with pulse lengths of 5 ps and 4 ps respectively and coincident at the entrance of the undulator. The accelerated fraction was 10 % with a mean energy of 117 MeV and a FWHM energy spread of 1.7 %. The accelerated pulse had a reduced rms pulse length of 1.7 ps owing to the fact that only the center part of the laser has a strong enough electric field to maintain resonance.

## ACCEPTANCES AND TOLERANCES

The final energy of the accelerated electrons is insensitive to most input parameters since the resonant energy is determined by the undulator tapering. Small deviations from the optimal parameters will cause fewer particles to be trapped and accelerated so the best figure of merit describing the performance is the fraction of particles accelerated. A study of the tolerances in the parameters which still allow for an acceptable accelerated fraction was performed by systematically varying the parameters from their optimal values in the simulation, and the results are listed in Table 4.

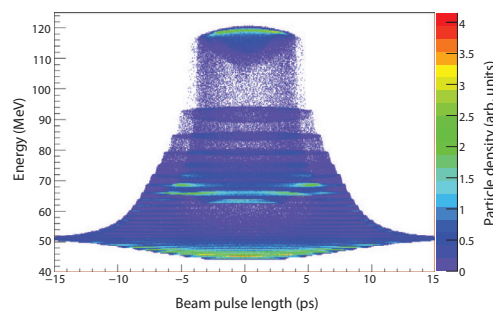


Figure 5: Output energy along the beam envelope for a time dependent simulation with the optimal parameters.

Restrictions on the input energy are limited by the ponderomotive bucket which is centered on the resonant energy. Particles injected much less than 1 MeV below the design input energy of 50 MeV are never trapped. On the other hand, particles injected above the resonant energy will be in resonance further along the undulator, and 10 % of the particles are still accelerated when injected 5 MeV above resonance.

Accelerated electrons steal energy from the laser and reduce the electric field available for acceleration. Too much laser depletion may lead to detrapping after a point in the undulator and reduce the final energy. Increasing the peak current from 100 A to 6000 A results in a reduction from 26 % captured beam to 20 %, and even for 11 kA, 10 % of the particles are still accelerated to the nominal final energy. This suggests a relatively high tolerance for beam loading.

Table 4: Parameter Tolerances

| Parameter      | 20% capture     | 10% capture     |
|----------------|-----------------|-----------------|
| Input energy   | 49.8 – 53.7 MeV | 49.1 – 54.9 MeV |
| Laser power    | > 440 GW        | > 370 GW        |
| Beam offset    | < 260 $\mu$ m   | < 480 $\mu$ m   |
| Peak current   | < 6 kA          | < 11 kA         |
| Rayleigh range | < 30 cm         | < 37 cm         |
| Focal position | -11.8 – 1.2 cm  | -16.8 – 7.7 cm  |

## CONCLUSIONS

The expected performance and tolerances of the undulator are encouraging. With the undulator constructed and tuned, attention has now turned to beam line and laser configurations. The undulator was transported to ATF, and initial beam line construction is under way.

This work was supported by DOE grant DE-FG02-92ER40693 and Defense Threat Reduction Agency award HDTRA1-10-1-0073.

## REFERENCES

- [1] A. Tremaine et al. in Proceedings of the 2011 Particle Accelerator Conference, New York, NY, 2011.
- [2] W. Kimura et al., *Phys. Rev. Lett.*, 92:054801, 2004.
- [3] P. Musumeci et al., *Phys. Rev. Lett.* 94:154801, 2005.
- [4] J.P. Duris, P. Musumeci, and R. K. Li, *Phys. Rev. ST Accel. Beams*, Inverse Free Electron Laser accelerator for advanced light sources, Accepted for publication, 2012.
- [5] J. A. Clarke, Oxford University Press, 2004.
- [6] T. Bizen, in Proceedings of the Eighth International Conference on Synchrotron Radiation Instrumentation, San Francisco, CA, 2003.
- [7] S. Reiche, K. Goldhammer, P. Musumeci in Proceedings of PAC07, Albuquerque, New Mexico, USA, IEEE, 2007.
- [8] J. Duris et al., in Proceedings of the 2011 Particle Accelerator Conference, New York, NY, 2011.